

# The vibrational excitations of glasses in the boson-peak region: application to borates

R. Vacher,<sup>1</sup> B. Rufflé, B. Hehlen, G. Guimbrètière, G. Simon & E. Courtens

Laboratoire des Colloïdes, Verres et Nanomatériaux, UMR 5587 CNRS, Université Montpellier II, F-34095 Montpellier Cedex 5, France

---

*There exists a special interest in investigating acoustical and optical vibrations of glasses in the one THz frequency region. The main experimental tools that are used to this effect are briefly discussed. The current understanding of the boson-peak vibrations and of their resonance with acoustic branches are explained. Specific new results on the origin of the boson peak and on the end of acoustic branches are presented for borates.*

---

## 1. Introduction

A main goal of the present paper is to explain in simple terms a question which is currently very much debated in the physics of glasses. The issue is that of the nature and properties of vibrational excitations at frequencies  $\nu \approx \Omega/2\pi$  of the order of 1 THz (or  $30 \text{ cm}^{-1}$ , or also  $\hbar\Omega \approx 4 \text{ meV}$ ). As shown below, these excitations are mainly of two types: *optic* ones, which in a molecular picture can be thought of as the more or less local vibrations of structural units, and *acoustic* ones which are approximately collective rigid translations of the same units. It is legitimate to ask why is this question of such interest. The profound reason derives from a series of observations from which a sequence of conclusions can be derived. It is worth following these steps one by one.

(i) First it is known that there are *excess vibrational modes* in most glasses, which occur at relatively “low” frequencies.<sup>(1)</sup> The existence of these quasi-harmonic modes is best seen in the low temperature ( $T$ ) specific heat  $C_p$  which shows a large “hump” when plotted as  $C_p/T^3$  versus  $T$ .<sup>(2)</sup> In the Debye model of thermal properties, the Debye value  $C_p^D$  is proportional to  $T^3$  and it only depends on the sound velocities.<sup>(3)</sup> One speaks of an excess because around the hump  $C_p$  is much larger than  $C_p^D$ . The hump typically peaks at a  $T_{\text{max}}$  between  $\sim 3$  and  $\sim 10 \text{ K}$ . The corresponding dominant thermal phonons are given by  $\hbar\nu \sim 5k_B T$ , with  $k_B$  the Boltzmann constant. This leads to a value of  $\nu$  typically of the order of 1 THz, which is what was meant by “low” frequencies above. Indeed, these are low compared to the usual optic modes in crystals. One remarks that the Debye density of acoustic modes  $Z^D(\omega)$  is simply proportional to  $\omega^2$ , which is the reason for the  $T^3$  law above. Note that we use  $\omega$  for spectral frequencies and

$\Omega$  for the frequency of specific modes. As opposed to  $Z^D(\omega)$ , the real density of vibrational states  $Z(\omega)$  shows a peak when plotted as  $Z(\omega)/\omega^2$  versus  $\omega$ . It is this particular feature which is called the *boson peak* (BP). This somewhat unfortunate name has been given because in spectroscopies of this spectral region, the  $T$  dependence of the strength of this feature follows the Bose–Einstein statistics characteristic of harmonic modes,<sup>(4)</sup> as opposed to structural relaxations which do not. The angular frequency at the BP maximum will be written  $\Omega_{\text{BP}}$ .

(ii) The second point is that *the energy in these excess vibrations does not propagate* like plane-wave acoustic modes would allow. This is known from the thermal conductivity  $\kappa(T)$ , which normally grows with some power of  $T$  at low  $T$ , but which starts to saturate, exhibiting an anomalous “plateau” in a logarithmic presentation of  $\kappa(T)$  versus  $T$ .<sup>(1)</sup> This plateau is observed at temperatures around the same  $T_{\text{max}}$ . Hence, not only are there more modes than just the normal acoustic ones, but also the acoustic modes have lost their propagating plane-wave character at  $\Omega_{\text{BP}}$ . One speaks of an *Ioffe–Regel* (IR)<sup>(5)</sup> crossover for acoustic modes, occurring at  $\Omega_{\text{IR}}$ . This crossover can be defined as the frequency at which the *energy* mean-free-path  $l$  becomes equal to only half the acoustic wavelength,  $l = \lambda/2$ .<sup>(6)</sup> This is really a limit for plane-wave like propagation. As shown explicitly below, one finds experimentally that  $\Omega_{\text{IR}} \approx \Omega_{\text{BP}}$ . This is now understood as due to the hybridisation of the acoustic modes resonating with the optic ones.<sup>(7,8)</sup> Hence, in the glasses for which the BP is sufficiently strong (which is the case for all glasses of technical interest), there should be no plane-wave-like acoustic modes left above  $\Omega_{\text{IR}}$ . One can say that the acoustic branch *terminates* at  $\Omega_{\text{IR}}$ : what was “low” frequency for optic modes has become a “very high” frequency for acoustic modes.

---

<sup>1</sup> Corresponding author. Email rene.vacher@univ-montp2.fr

(iii) The special interest in this spectral region arises when one considers the *typical scale* at which this occurs. Extrapolating the wavelength of acoustic modes to  $\Omega_{\text{IR}}$ , one typically finds values  $\lambda \approx 5$  nm. Of course, the BP vibrations need not be exactly of the same extent. They could be of smaller extent and nevertheless modify the acoustic modes owing to the strong resonance with them. In any case, the BP vibrations and their interaction with acoustic waves are likely to give information about the structure of glasses at medium to long range scales, about which so little is known otherwise. The most promising approach will presumably be to check the validity of simulated structures by calculating from them the observed BP spectra. This is expected to become an exacting test for structures. To our knowledge, such large scale simulations of the BP-region have not yet been achieved for the full collection of spectroscopies which have now been applied to this problem. To summarise, it is expected that detailed studies of the BP will be central to the understanding of the disorder particular to glasses.

In the case of borates, one has an excellent example in which vibrations have given decisive structural information which was difficult to obtain with classical structural tools.<sup>(9)</sup> This is the question of the existence and the number of boroxol rings in vitreous boron oxide, v-B<sub>2</sub>O<sub>3</sub>. The breathing motion of the rings produces a narrow Raman scattering feature at 808 cm<sup>-1</sup><sup>(10)</sup> whose relative strength has recently been used in relation with simulations<sup>(11)</sup> to definitively establish the fraction of boroxol rings in v-B<sub>2</sub>O<sub>3</sub>. In the case of the BP, it can be considered as having its origin in the lowest frequency optic-like vibrations of structural units. These generally are the rigid librations, which by a cog-wheel effect couple with translations. In the borates, the structural units are quite varied. They can be the BO<sub>3</sub> triangles, the B<sub>3</sub>O<sub>3</sub> boroxols, and the BO<sub>4</sub> tetrahedra, among others. Hence, the study of the BP should be of special interest for borate glasses.

The plan of the paper will be the following. Section 2 gives a brief summary of the situation in borates and in the course of the development it presents the various experimental approaches that are traditionally used to gain information about the BP and the end of acoustic branches. In particular, it emphasises that each spectroscopy has its specific selection rules, explaining that apparently “different” BPs might be observed in diverse experiments. Section 3 describes a recent progress achieved in the observation of low lying optical modes of v-B<sub>2</sub>O<sub>3</sub> using an alternate spectroscopy, namely hyper-Raman scattering. It also describes advances in the observation of acoustic excitations in lithium diborate that became possible by pushing the limits of Brillouin scattering spectroscopies, whether using x-ray or visible light

excitation. Finally, Section 4 summarises the present understanding of the BP and of its hybridisation with the acoustic modes.

## 2. The boson peak and high frequency sound in borate

An unbiased observation of the density of states (DOS)  $Z(\omega)$  is provided by measurements of the specific heat  $C_p$  at low temperatures  $T$ . At sub-helium  $T$ , one observes a contribution to  $C_p$  which is linear in  $T$ ,  $C_p = c_1 T$ . It is explained by two-level systems.<sup>(12)</sup> As  $T$  is raised, one expects to find in addition the Debye contribution which can be written  $C_D = c_3^D T^3$ . The value of  $c_3^D$  should be given by the sound velocities. However, it has been known for a long time that an adjustment of the low- $T$  specific heat of glasses to  $C_p = c_1 T + c_3 T^3$  leads to values of  $c_3$  significantly larger than the Debye  $c_3^D$ .<sup>(12)</sup> This apparent discrepancy has recently been very well explained.<sup>(13)</sup> It is due to the low frequency tail of the BP-modes, whose density varies approximately as  $\omega^4$ , leading to an extra term  $c_5 T^5$  in the specific heat. It has been shown that for v-B<sub>2</sub>O<sub>3</sub>, as well as for a series of alkali borates, adjusting  $C_p$  to  $c_1 T + c_3 T^3 + c_5 T^5$  leads to  $c_3 \equiv c_3^D$ . This confirms the validity of the Debye model for the acoustic mode contribution. It also shows that the low- $\omega$  onset of the BP DOS is well approximated by  $Z(\omega) \propto \omega^4$ . As  $T$  is further raised, a plot of  $C_p/T^3$  goes then through a maximum at  $T_{\text{max}}$  which evidently ought to be related to the maximum in  $Z(\omega)/\omega^2$ , which we have called  $\Omega_{\text{BP}}$ . It can indeed be shown that  $\hbar\Omega_{\text{BP}} = ak_B T_{\text{max}}$ , where  $a$  is a constant that depends slightly on the exact shape of the reduced distribution  $Z(\omega)/\omega^2$ . The latter difficulty arises because the contribution to  $C_p$  of a given mode of frequency  $\Omega$  does not set in sharply in function of  $T$ , but rather gradually, smoothed by the Bose population factor  $n(\Omega)$ .<sup>(3)</sup> The value of  $a$  is typically around 5 or 6. Since  $k_B T$  at 1 K corresponds to a frequency of 20.86 GHz, this value of  $a$  gives  $\Omega_{\text{BP}}/2\pi \approx 21$  cm<sup>-1</sup> for v-B<sub>2</sub>O<sub>3</sub> in which  $T_{\text{max}} \approx 5.2$  K,<sup>(14)</sup> which is a reasonable result.<sup>(15,16)</sup> Although the measurement of  $C_p$  gives an unbiased access to  $Z(\omega)$ , it is not a direct one. For this reason, and also because quality low- $T$  specific heat measurements are demanding experiments, one finds in the literature many more measurements of BPs by spectroscopic techniques.

The vast majority of BP observations have in fact been made using Raman scattering (RS). The difficulty here is that one does not know for sure what is the Raman activity of the modes involved in producing the BP. As explained in Ref. 17, the Stokes intensity can be written as a sum over bands

$$I(\omega) = \sum_b C_b Z_b(\omega) [1 + n(\omega)] / \omega \quad (1)$$

where  $b$  is a band index,  $Z_b$  is the DOS of the particular

band, and  $C_b$  is a light-vibration coupling coefficient. For simple Raman-active optic modes,  $C_b$  should be a constant, only depending on the band, but in more complicated cases it might depend on the modes within a given band. This is now well understood for vitreous silica,  $v\text{-SiO}_2$ . The BP is there related to rigid librations of  $\text{SiO}_4$  tetrahedra, as known from inelastic neutron scattering,<sup>(18)</sup> hyper-Raman scattering,<sup>(19)</sup> or also simulations.<sup>(20)</sup> Undistorted  $\text{SiO}_4$  tetrahedra are optically isotropic so that their pure librations are *inactive* in RS. Hence, the observed RS BP must be related either to small tetrahedra distortions or to the coupling of librations with Raman-active translations. In either case, it is obvious that the coupling to light depends then on the environment of the librating tetrahedra, and thus on the particular mode frequency. It became customary to use in this case an *effective* frequency dependent coupling coefficient  $C(\omega)$ , as reported in Ref. 21. For the borates, there are great many reports of BP observations with Raman scattering. For  $v\text{-B}_2\text{O}_3$ , the BP depends significantly on the water content and on the fictive temperature of the glass.<sup>(22,23)</sup> In series of alkali borates, one observes that  $\Omega_{\text{BP}}$  evolves rapidly with the alkali concentration.<sup>(15,24–27)</sup> Mixing with alkali produces  $\text{BO}_4$  tetrahedra at the expense of  $\text{B}_3\text{O}_3$  rings. The trend on  $\Omega_{\text{BP}}$  is easily understood as tetrahedra must have higher librational frequencies. They are also much less Raman active, so that the BP intensity drops rapidly with increasing concentration.<sup>(25,27)</sup> It is clear that in situations where there are several different structural units, such as  $\text{BO}_3$  triangles,  $\text{B}_3\text{O}_3$  boroxols, and  $\text{BO}_4$  tetrahedra, Equation (1) must be used with all due care, and that a single  $C(\omega)$  might not be physically significant.

The DOS entering in Equation (1) is most often obtained from inelastic neutron scattering (INS) experiments. The first important point in INS is that for borates the experiments must be performed with samples made of isotopically pure  $^{11}\text{B}$ . Indeed, the boron isotope  $^{10}\text{B}$  has an enormous thermal neutron absorption coefficient, incompatible with INS experiments. The second point is that one must consider carefully the meaning of the INS structure factor  $S(Q, \omega)$ , where  $Q$  is the scattering vector. It is incorrect to assume that  $S(Q, \omega)$  is simply proportional to the density of states,  $S(Q, \omega) \propto Z(\omega)[1+n(\omega)]/\omega$ , as it would be in incoherent scattering. Indeed,  $^{11}\text{B}_2\text{O}_3$  is a coherent scatterer, and librations imply correlated motions of nearby units. This is clearly a second difficulty, besides the one mentioned above, in using Equation (1) for determining a single physically meaningful light-vibration coupling coefficient  $C(\omega)$ .  $S(Q, \omega)$  has been analysed in detail for  $v\text{-B}_2\text{O}_3$ , with the result that one can extract from the INS signal an incoherent part, also named *out-of-phase* in Ref. 28. This incoherent part matches the RS signal, implying that really

$C(\omega) \propto \omega^0$  in this case. The coherent, or *in-phase* part, shows a BP at a lower frequency than the RS BP. It appears that no other INS results on borate glasses are available to date. On the other hand, neutron scattering was used extensively to investigate the structure of these glasses, e.g. in Refs 9, 29, 30, but this is a different subject.

The observation of hypersonic acoustic modes and of their broadening is most conveniently achieved with Brillouin scattering (BS) of electromagnetic waves. In these experiments, the momentum transfer  $Q$  is fixed by the experimental geometry,  $Q = \mathbf{k}_i - \mathbf{k}_f$ , where  $\mathbf{k}_i$  and  $\mathbf{k}_f$  are the initial and final momentum of the photons, respectively. Energy conservation implies that one observes excitations at a frequency  $\omega = \omega_i - \omega_f$  where  $\omega_{i,f}$  are the photon frequencies. With this choice of sign, negative  $\omega$  means that an excitation is annihilated in the material, corresponding to the anti-Stokes side of the spectrum. One should note that the velocity of sound  $v$  is much smaller than the velocity of light  $c$ , and that both play an essential role in the experiment since  $\omega_{i,f} = ck_{i,f}$  while for a sound wave  $\Omega = vQ$ . Since  $c \gg v$ , it follows that  $k_f \approx k_i$ . For incident radiation of a given frequency, backscattering gives the highest achievable  $Q$ -value, which is  $\approx 2k_i$ . With visible light excitation, this limits  $Q$  to typically  $\sim 0.04 \text{ nm}^{-1}$ , and thus the highest observable sound frequency  $\Omega$ , which depends on  $v$ , typically ranges from  $\sim 20$  to  $\sim 40 \text{ GHz}$  for glasses. To observe higher frequency acoustic modes, it is necessary to use a higher frequency excitation. This has been attempted in silica using the second-harmonic of visible lasers and also synchrotron produced UV excitation,<sup>(31,32)</sup> but this is rapidly thwarted by the sample absorption that limits the definition of  $Q$ . This approach allows at most an increase of  $Q$  by a factor of 3 to 4. Much higher frequencies can be achieved with x-rays, which then require the very high energy and angular resolutions that are only possible at advanced synchrotron sources. One speaks then of inelastic x-ray scattering (IXS).<sup>(33)</sup> If it is of interest to measure the linewidth of the scattered spectrum,  $\Gamma$ , it is then the resolution of the monochromator and analysers that is the limiting factor in IXS. The highest practical resolution to date has been achieved with  $21.75 \text{ keV}$  radiation (corresponding to  $\sim 5.3 \times 10^{18} \text{ Hz}$ ), and it is  $1.5 \text{ meV}$  full width (or  $\sim 0.36 \text{ THz}$ ).<sup>(34)</sup> This radiation penetrates sufficiently into samples of low atomic number to allow for many significant BS experiments. At such a high incident energy,  $k_i$  is *much larger* than any  $Q$  of interest in the glass. One is then in the opposite limit where one wants to work close to forward scattering to achieve at best  $Q \sim 1 \text{ nm}^{-1}$ . This is in the range of the IR-crossover wavevector,  $q_{\text{IR}}$ , of most glasses. Unfortunately, there exists no BS technique to access the potentially interesting region between  $\sim 0.1$  and  $1 \text{ nm}^{-1}$ . In performing IXS experiments, it is therefore

of prime interest to select materials for which  $q_{\text{IR}}$  is expected to be as large as possible, in order to be able to explore the region between  $1 \text{ nm}^{-1}$  and  $q_{\text{IR}}$ .

Up to now, among borates, only  $v\text{-B}_2\text{O}_3$ ,<sup>(35)</sup>  $\text{Li}_2\text{O-4B}_2\text{O}_3$ ,<sup>(36)</sup> and  $\text{Li}_2\text{O-2B}_2\text{O}_3$ ,<sup>(36,37)</sup> have been investigated with IXS. In all three cases, a strong saturation of the linear dependence of  $\Omega$  on  $Q$  was observed. It was interpreted as the manifestation of the IR-crossover. In that saturation regime, the full width  $\Gamma$  of a damped harmonic oscillator (DHO) lineshape adjusted to the spectrum is almost equal to the frequency  $\Omega$  (both in angular frequency units). In fact, the definition of the crossover given above,  $l=\lambda/2$ , implies that  $\Gamma=\Omega/\pi$  when one uses  $\Gamma=v/l$  and  $f=\lambda v$ . The condition  $\Gamma=\Omega/\pi$  occurs quite a bit before the saturation of  $\Omega(Q)$ , indicating that the saturation regime is far beyond the IR-crossover. We return to this in Section 3.2.

The above summarises the main experimental techniques that are presently available to investigate the frequency region of interest. As shown, there exists so far relatively little information on the boson peak region of borate glasses, except maybe for the always abundant Raman scattering literature.

### 3. Recent progress

#### 3.1. Hyper-Raman scattering from boron oxide

Hyper-Raman scattering (HRS) is a nonlinear optical spectroscopy in which two incident photons simultaneously create or destroy one quantised excitation in the material to produce one scattered photon.<sup>(38,39)</sup> The scattered photon is thus at an energy equal to twice that of the incident photon minus or plus the energy of the excitation. HRS obeys selection rules that are different from those of RS.<sup>(40)</sup> Therefore, the two techniques can advantageously be combined to identify which motions of the structural units produce the vibrational spectra, and in particular which motions are responsible for the BP. This was already described for the BP of  $v\text{-SiO}_2$ .<sup>(19)</sup> In the case of  $v\text{-B}_2\text{O}_3$ , the spectra can be indexed in terms of vibrations of structural units consisting principally of  $\text{B}_3\text{O}_3$  rings and  $\text{BO}_3$  triangles, in about 1:1 ratio.<sup>(11)</sup>

We recently showed that the BP observed both in RS and HRS (Figure 1) in  $v\text{-B}_2\text{O}_3$  is produced by out-of-plane rigid librational motions of the structural units.<sup>(41)</sup> With flat structural units like these, out-of-plane librations are active both in RS and HRS, so that one would at first expect that the two BPs have somehow similar intensities. As found from an analysis of Figure 1, this turns out not to be the case. To compare the RS and HRS intensities, it is necessary to make use of a reference. Such a reference is provided by the  $808 \text{ cm}^{-1}$  narrow peak in both spectra. As already indicated above, this peak corresponds to the breathing motion of the  $\text{B}_3\text{O}_3$  rings.<sup>(10)</sup> This is a local mode that should scatter

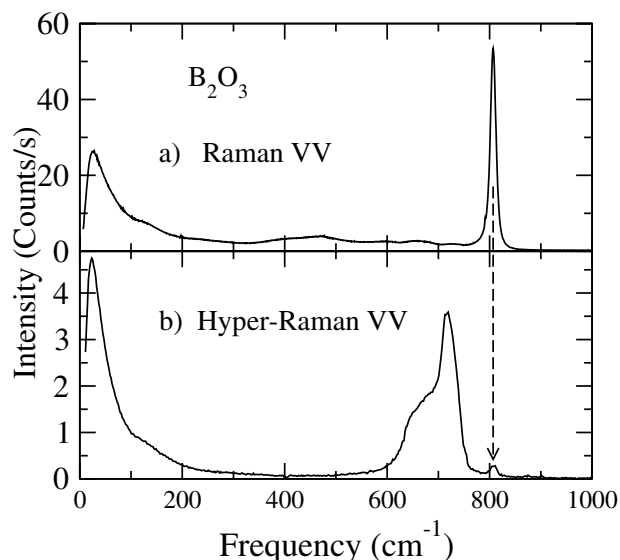


Figure 1. Raman and hyper-Raman intensities observed in  $90^\circ$  scattering and in VV polarisation on  $v\text{-B}_2\text{O}_3$  at room temperature. The vertical line shows the position of the  $808 \text{ cm}^{-1}$  breathing mode of the  $\text{B}_3\text{O}_3$  rings which is a small peak in the HRS spectrum on this scale. The frequency of the BP is slightly lower in HRS than in RS

equally well in both spectroscopies. In other words, it sets the scale to compare Figure 1(b) to Figure 1(a). It becomes then obvious that the BP scatters much more strongly in HRS than in RS, by nearly two orders of magnitude. As explained elsewhere, this enhancement of the HRS BP is produced by the coherence of the librational motions of many connected units.<sup>(41)</sup> For reasons of symmetry of the polarisability and hyper-polarisability tensors, the coherence affects differently the RS and HRS BPs. In fact, the RS BP signal appears to be dominated by incoherent scattering, as its shape matches well the out-of-phase component extracted from INS.<sup>(28)</sup> On the other hand, the HRS BP is slightly shifted to lower frequencies owing to the coherent motions. It should not be confused with the INS in-phase signal<sup>(28)</sup> which is produced by Umklapp scattering of the acoustic modes and which for that reason mimics the BP although it does not really reflect the BP density of states.

The reader will also have noticed the group of modes located between  $600$  and  $750 \text{ cm}^{-1}$  in Figure 1(b). These other strong modes are due to scattering by cooperative infrared-active LO-TO motions of the structural units. The particular motions leading to this group of modes are opposite displacements of B and O atoms perpendicular to the plane of the structural units.<sup>(41)</sup> The sharpest peak in this group can be assigned to the boroxols. It is interesting to remark that the BP and these other collective modes have similar activities.

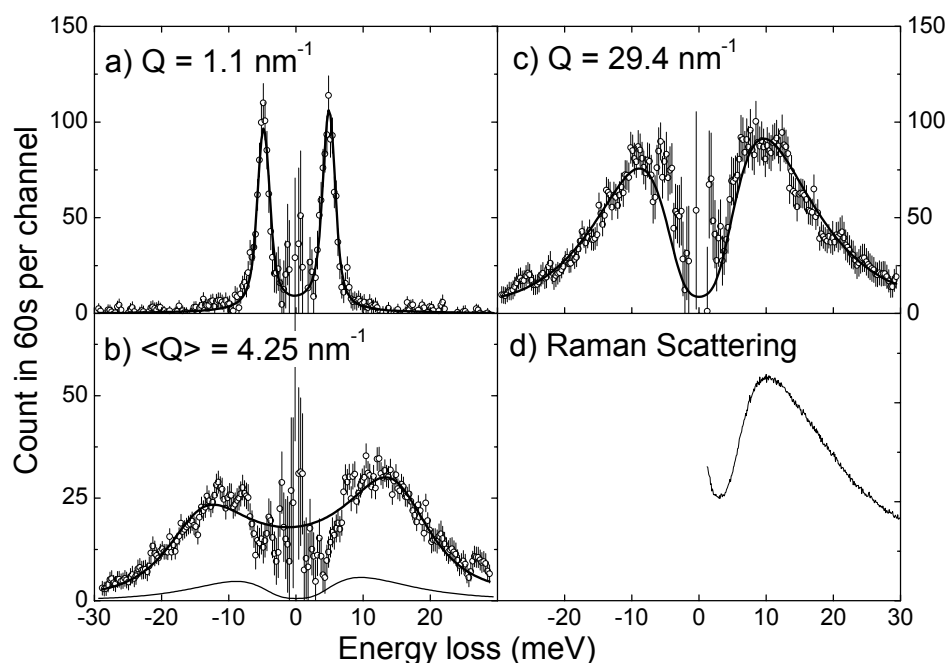


Figure 2. (a)–(c) The inelastic part of IXS spectra observed on  $\text{Li}_2\text{O}-2\text{B}_2\text{O}_3$  at 573 K for three values of  $Q$ . In (a), the two peaks are produced by usual sound waves, while (b) is for  $Q$  well above  $q_{\text{IR}}$  so that the sound excitations become diffusive. In panel (c), the signal is dominated by the optic modes forming the boson peak. The solid lines in (a)–(c) are explained in the text. The thin line in (b) is an estimate of the optic-mode contribution to that spectrum. Panel (d) shows the Stokes side of the boson peak measured in RS. Its shape is very similar to the IXS spectrum in panel (c)

We hope that the observations of the relative strength of these BPs will stimulate large scale simulations aimed at obtaining quantitative estimates of the size of the coherently vibrating regions. This will presumably require a realistic model of the structure. This of course would be a major contribution towards clarifying the medium to long range order of these glasses.

### 3.2. The acoustic modes and IR-crossover of lithium diborate

We have recently investigated in detail, using IXS, the very high frequency acoustic modes of lithium diborate glass,  $\text{Li}_2\text{O}-2\text{B}_2\text{O}_3$ .<sup>(42)</sup> A few typical spectra are illustrated in Figure 2. The left-hand side of Figure 2 shows Brillouin spectra of acoustic modes in two extreme situations, well below crossover in (a) and well above it in (b). Figure 2(a) is at the lowest usable scattering vector,  $Q=1.1 \text{ nm}^{-1}$ , where one observes a narrow Brillouin doublet corresponding to sound waves of frequency  $\nu \approx 1 \text{ THz}$ . The apparent width in Figure 2(a) is essentially set by the instrumental resolution. As the scattering angle is increased, one first observes the usual linear increase of  $\Omega$  with  $Q$ , accompanied by a rather unusual very fast increase of the linewidth  $\Gamma$ . The latter is obtained by adjusting the Brillouin spectra to the DHO lineshape convoluted with the instrumental function. Such DHO adjust-

ments are shown by the solid lines in Figures 2(a)–(b). The initial increase of  $\Gamma$  with  $Q$  is approximately proportional to  $Q^4$ . This is observed up to  $Q \approx 1.8 \text{ nm}^{-1}$ , beyond which the fast increase in  $\Gamma$  slowly saturates. As explained above, the  $Q$  value at which  $\Gamma/\pi = \Omega$  is used as definition of the IR-crossover,  $q_{\text{IR}}$ . We find for the crossover frequency  $\Omega_{\text{IR}}/2\pi = 2.1 \text{ THz}$ , at a wavevector  $q_{\text{IR}} = 2.1 \text{ nm}^{-1}$ . Beyond this crossover, the spectrum continues to broaden, while  $\Omega$  starts to saturate. This is the other extreme case illustrated in Figure 2(b). The signal of Figure 2(b) is still mostly of acoustic origin, as explained below. However, being so far above crossover, it is not produced at all by plane waves, but rather by diffusive excitations. We recall that the DHO is the lineshape resulting from the scattering of radiation by exponentially damped plane waves. We have noticed that the DHO adjustment becomes progressively poorer as  $Q$  increases beyond  $q_{\text{IR}}$ . This can be seen in Figure 2(b), particularly in the central region of the spectrum, from about  $-12$  to  $+12 \text{ meV}$ . The origin of this departure from the DHO is now well understood.<sup>(43–45)</sup> It reflects the fact that this line shape is essentially *inhomogeneous*, being the sum of many individual excitations with ill defined wave vectors. The central dip in the observed spectrum of Figure 2(b) occurs because at small  $\Omega$  the wave vector of the sound waves is well defined and small. Thus excitations of small frequency just cannot contribute to the scattering at this large experimental  $Q$  value.

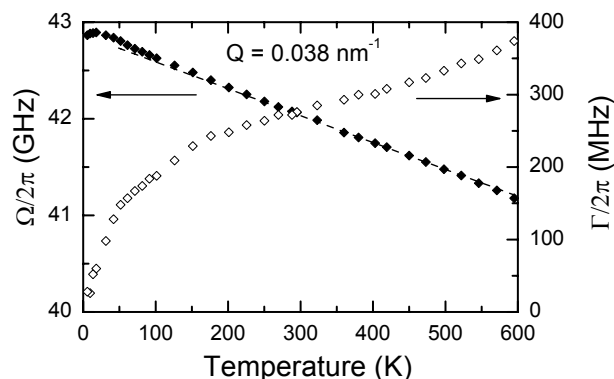


Figure 3. The temperature dependence of the frequency and full width of the longitudinal acoustic mode measured in Brillouin light scattering on  $\text{Li}_2\text{O}-2\text{B}_2\text{O}_3$  at  $0.038 \text{ nm}^{-1}$ . The error bars are smaller than the symbols

As  $Q$  is further increased, the signal becomes progressively dominated by optic-like modes. This is illustrated in Figure 2(c) which shows essentially the BP whose maximum is located at  $\Omega_{\text{BP}}/2\pi = 2.2 \text{ THz}$ . This signal can be compared to the RS BP observed on the same glass, as shown in Figure 2(d). The fitted line in Figure 2(c) is a log-normal, a function which has been advocated for the BP.<sup>(46)</sup> The intensity of the optic-like scattering is proportional to  $Q^2$  when due account is taken of the x-ray atomic form factors.<sup>(42)</sup> Extrapolating the optic-like signal to the  $Q$ -value of Figure 2(b) leads to the thin line drawn there. This confirms that the scattering at  $4 \text{ nm}^{-1}$  is still dominated by acoustic-like modes. To summarise, the approach of  $(q_{\text{IR}}, \Omega_{\text{IR}})$  from below is characterised by a very fast increase of  $\Gamma \propto \Omega^4$ . This is the region where specific-heat measurements reveal a contribution in  $Z(\omega) \propto \omega^4$ , as explained above. The two must obviously be related. Further,  $\Omega_{\text{IR}}$  nearly coincides with the maximum of the BP,  $\Omega_{\text{IR}} \approx \Omega_{\text{BP}}$ , emphasising a common origin.

It is also of interest to examine what happens to  $\Omega$  and  $\Gamma$  at lower  $Q$ s. Values around  $0.04 \text{ nm}^{-1}$  and below can be investigated by Brillouin scattering of light (BLS) in the visible region of the spectrum. The results of such an investigation, using the backscattering geometry and the green argon laser line as excitation, are shown in Figure 3.<sup>(47)</sup> These have been obtained with a very high resolution Fabry–Perot spectrometer of the type described in Ref. 48. This instrument includes a reference signal used for frequency calibration, a multiple pass planar interferometer acting as a filter, and in series a spherical interferometer that provides the very high resolution. With such an instrument the error bars in Figure 3 are smaller than the size of the data points. We observe that the sound velocity  $\Omega/Q$  decreases almost linearly with increasing temperature  $T$ . This is typical of the anharmonic coupling of sound with thermal vibrations, an effect

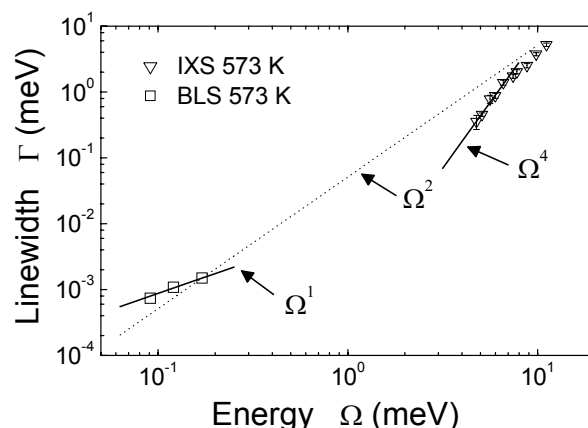


Figure 4. The frequency dependence of the linewidths measured on  $\text{Li}_2\text{O}-2\text{B}_2\text{O}_3$  with BLS and INS at 573 K. The solid lines are guides to the eye emphasising the different regimes observed in the two spectroscopies. The dotted line is just there to show that an  $\Omega^2$  dependence would be a very poor approximation

which is seen in crystals as well as in glasses.<sup>(49)</sup> The relative slope,  $d\ln\Gamma/d\ln\Omega$ , allows one to estimate the anharmonic contribution to the Brillouin linewidth provided the mean relaxation time of the thermal vibrations is known.<sup>(50)</sup> Making reasonable estimates, one finds that, although anharmonicity dominates the behaviour of  $\Omega(T)$ , its contribution to  $\Gamma$  is negligible in this frequency region compared to the observed broadening.<sup>(47)</sup>

The linewidth was measured with BLS at several scattering angles, i.e. at several values of  $Q$  and thus of  $\Omega$ . As shown in Figure 4, we find around room temperature that  $\Gamma \propto \Omega$ . A line in  $\Omega^1$  is traced through these points. This behaviour is characteristic of damping produced by thermally activated relaxation (TAR) of “structural defects” at frequencies in the region of the maximum damping.<sup>(51)</sup> This is due to the fact that TAR gives  $\Gamma \propto \Omega^2\tau/(1+\Omega^2\tau^2)$ , where  $\tau$  is a characteristic relaxation time of the defects. In general there is a broad distribution of  $\tau$  which widens the region where  $\Gamma \propto \Omega$ .

The measured IXS linewidths are also shown in Figure 4. The onset of crossover in  $\Omega^4$  applies to the first five data points. It is followed by the progressive saturation that has been described above. One concludes that the behaviour of  $\Gamma(\Omega)$  is complex. It cannot be approximated by a single power law  $\Gamma \propto \Omega^2$ , as illustrated by the dotted line. Beyond  $\Omega_{\text{IR}}$ , the linewidth cannot be strictly defined since DHO fits become progressively meaningless. However, other workers have observed that enforcing fits to DHO, the linewidth varies then approximately in  $\Omega^2$ . All this emphasises that different mechanisms producing the broadening might dominate in different frequency regions. The variation of  $\Gamma$  with  $\Omega$  is fastest in the very rapid increase below the IR crossover.

## 4. Summary and outlook

The main facts emerging from the above presentation are the following:

- (i) There exists an IR crossover beyond which acoustic modes cease to propagate as plane waves. This has now been clearly demonstrated in two cases, permanently densified silica glass d-SiO<sub>2</sub><sup>(45)</sup> and Li<sub>2</sub>O–2B<sub>2</sub>O<sub>3</sub>. However, we have shown recently that such a crossover occurs in nearly all glasses on which we have the necessary experimental information.<sup>(42)</sup>
- (ii) There also exists a boson peak which is produced by excess modes of low frequency. These excess modes appear to be of optic origin and involve collective motions of structural units, as found for v-SiO<sub>2</sub><sup>(18)</sup> and B<sub>2</sub>O<sub>3</sub>.<sup>(41)</sup>
- (iii) With the definition given here for  $\Omega_{\text{IR}}$ , the IR crossover nearly coincides with  $\Omega_{\text{BP}}$ . This is shown above for Li<sub>2</sub>O–2B<sub>2</sub>O<sub>3</sub>, but it is also found for all sufficiently strong glasses when  $\Omega_{\text{IR}}$  is known.<sup>(42)</sup> These “strong” glasses are these where the BP is well developed.<sup>(52)</sup>
- (iv) The approach of the crossover from below is characterised by a very rapid increase of the acoustic damping with the acoustic frequency. This was shown in the needed details for d-SiO<sub>2</sub><sup>(45)</sup> and Li<sub>2</sub>O–2B<sub>2</sub>O<sub>3</sub>.<sup>(42)</sup> It seems related to the rapid increase of  $Z(\omega) \propto \omega^4$  at similar frequencies. This points to a resonant interaction between the acoustic modes and the excess optic ones. It strongly supports the concept that the position and shape of the boson peak itself, and in particular the fact that  $\Omega_{\text{BP}} \approx \Omega_{\text{IR}}$ , result from the hybridisation of acoustic and optic modes.<sup>(7)</sup>

The existence of the excess vibrational excitations at low frequencies, and their coincidence with the end of acoustic branches, are not specific to borates. However, as shown above, borates have offered some very nice test cases to explore these facts. This will be worth pursuing, particularly in view of the structural modifications that can be produced in a controlled fashion in borates, for example by mixing boron oxide with alkali oxides. This will allow in the near future to perform what could be called some “creative” spectroscopy in which specific structural changes are performed to follow their influence on the spectral properties.

## References

1. Zeller, R. C. & Pohl, R. O. *Phys. Rev. B*, 1971, **4**, 2029.
2. *Amorphous Solids: Low Temperature Properties*, edited by W. A. Phillips, Springer-Verlag, Berlin, 1981.
3. *Introduction to Solid State Physics*, C. Kittel, Wiley, New York, Fifth Ed., 1976.
4. Stolen, R. H. *Phys. Chem. Glasses*, 1970, **11**, 83.
5. Ioffe, A. F. & Regel, A. R. *Prog. Semicond.*, 1960, **4**, 237.
6. This definition of the crossover is identical to that used, e.g. in Taraskin, S. N. & Elliott, S. R. *J. Phys.: Condens. Matter*, 1999, **11**, A219, as these authors write  $l_{\text{IR}} = \lambda_{\text{IR}}$ , where  $l_{\text{IR}}$  is defined as the amplitude mean free path, which is twice the energy mean free path.
7. Gurevich, V. L., Parshin, D. A. & Schober, H. R. *Phys. Rev. B*, 2003, **67**, 094203.
8. Klinger, M. I. & Kosevich, A. M. *Phys. Lett. A*, 2002, **295**, 311.
9. Hannon, A. C., Grimley, D. I., Hulme, R. A., Wright, A. C. & Sinclair, R. N. *J. Non-Cryst. Solids*, 1994, **177**, 99.
10. Galeener, F. L., Lucovsky, G. & Mikkelsen, Jr. J. C. *Phys. Rev. B*, 1980, **22**, 3983.
11. Umari, P. & Pasquarello, A. *Phys. Rev. Lett.*, 2005, **34**, 137401.
12. Pohl, R. O. in Ref. 2., p 27.
13. Ramos, M. A. *Phil. Mag.*, 2004, **84**, 1313.
14. Perez-Enciso, E., Ramos, M. A. & Vieira, S. *Phys. Rev. B*, 1997, **56**, 32.
15. Lorosch, J., Couzi, M., Pelous, J., Vacher, R. & Levasseur, A. *J. Non-Cryst. Solids*, 1984, **69**, 1.
16. Brodin, A., Borjesson, L., Engberg, D., Torell, L. M. & Sokolov, A. P. *Phys. Rev. B*, 1996, **46**, 11511.
17. Shuker, R. & Gammon, R. W. *Phys. Rev. Lett.*, 1970, **24**, 222.
18. Buchenau, U., Prager, M., Nucker, N., Dianoux, A. J., Ahmad, N. & Phillips, W. A. *Phys. Rev. B*, 1986, **34**, 5665.
19. Hehlen, B., Courtens, E., Vacher, R., Yamanaka, A., Kataoka, M. & Inoue, K. *Phys. Rev. Lett.*, 2000, **84**, 5355.
20. Taraskin, S. N. & Elliott, S. R. *Phys. Rev. B*, 1997, **56**, 8605.
21. Fontana, A., Dell’Anna, R., Montagna, M., Rossi, F., Viliani, G., Ruocco, G., Sampoli, M., Buchenau, U. & Wischniewski, A. *Europhys. Lett.*, 1999, **47**, 56.
22. Surotsev, N. V., Wiedersich, J., Batalov, A. E., Novikov, N. V., Ramos, M. A. & Rossler, E. *J. Chem. Phys.*, 2000, **113**, 5891.
23. Surotsev, N. V., Shebanin, A. P. & Ramos, M. A. *Phys. Rev. B*, 2003, **67**, 024203.
24. Kojima, S. & Kodama, M. *Physica B*, 1999, **263–264**, 336.
25. Baranov, A. V., Perova, T. S., Petrov, V. I., Vij, J. K. & Nielsen, O. F. *J. Raman Spectrosc.*, 2000, **31**, 819.
26. Kojima, S., Novikov, V. N. & Kodama, M. *J. Chem. Phys.*, 2000, **113**, 6344.
27. Denisov, Yu. V. & Zubovich, A. A. *Glass Phys. Chem.*, 2003, **29**, 345.
28. Engberg, D., Wischniewski, A., Buchenau, U., Borjesson, L., Dianoux, A. J., Sokolov, A. P. & Torell, L. M. *Phys. Rev. B*, 1998, **58**, 9087.
29. Johnson, P. A. V., Wright, A. C. & Sinclair, R. N. *J. Non-Cryst. Solids*, 1982, **50**, 281.
30. Majerus, O., Cormier, L., Calas, G. & Soper, A. K. *Physica B*, 2004, **350**, 58.
31. Masciovecchio, C., Gessini, A., Di Fonzo, S., Comez, L., Santucci, S. C. & Fioretto, D. *Phys. Rev. Lett.*, 2004, **92**, 247401.
32. Benassi, P., Caponi, S., Eramo, R., Fontana, A., Giugni, A., Nardone, M., Sampoli, M. & Viliani, G. *Phys. Rev. B*, 2005, **71**, 172201.
33. Sette, F., Krisch, M. H., Masciovecchio, C., Ruocco, G. & Monaco, G. *Science*, 1998, **257**, 1550.
34. Verbeni, R., Sette, F., Krisch, M. H., Bergmann, U., Gorges, B., Halcousis, C., Martel, K., Masciovecchio, C., Ribois, J. F., Ruocco, G. & Sinn, H. *J. Synchrotron Rad.*, 1996, **3**, 62.
35. Matic, A., Borjesson, L., Ruocco, G., Masciovecchio, C., Mermet, A., Sette, F. & Verbeni, R. *Europhys. Lett.*, 2001, **54**, 77.
36. Matic, A., Engberg, D., Masciovecchio, C. & Borjesson, L. *Phys. Rev. Lett.*, 2001, **86**, 3803.
37. Borjesson, L., Matic, A., Engberg, D. & Masciovecchio, C. ESRF experimental report HS-1147, 23/2/2000.
38. Terhune, R. W., Maker, P. D. & Savage, C. M. *Phys. Rev. Lett.*, 1965, **14**, 681.
39. Denisov, V. N., Marvin, B. N. & Podopedov, V. B. *Phys. Rep.*, 1987, **151**, 1.
40. Cyvin, S. J., Rauch, J. E. & Decius, J. C. *J. Chem. Phys.*, 1965, **43**, 4083.
41. Simon, G., Hehlen, B., Courtens, E., Longueteau, E. & Vacher, R. *Phys. Rev. Lett.*, 2006, **96**, 105502.
42. Ruffle, B., Guimbretiere, G., Courtens, E., Vacher, R. & Monaco, G. *Phys. Rev. Lett.*, 2006, **96**, 045502.
43. Vacher, R., Courtens, E. & Foret, M. *Phil. Mag. B*, 1999, **79**, 1763.
44. Rat, E., Foret, M., Courtens, E., Vacher, R. & Arai, M. *Phys. Rev. Lett.*, 1999, **83**, 1355.
45. Ruffle, B., Foret, M., Courtens, E., Vacher, R. & Monaco, G. *Phys. Rev. Lett.*, 2003, **90**, 095502.
46. Malinovsky, V. K., Novikov, V. N., Parshin, P. P. & Sokolov, A. P. *Europhys. Lett.*, 1990, **11**, 43.
47. Guimbretiere, G. Doctoral Thesis, University of Montpellier 2, France, Dec. 2005.
48. Vacher, R., Sussner, H. & v. Schickfus, M. *Rev. Sci. Instrum.*, 1980, **51**, 88.
49. Claytor, T. N. & Sladek, R. J. *Phys. Rev. B*, 1978, **18**, 5842.
50. Vacher, R., Courtens, E. & Foret, M. *Phys. Rev. B*, 2005, **72**, 214205.
51. Hunklinger, S. & Arnold, W. in *Physical Acoustics*, Vol. NII, W. P. Mason & R. N. Thurston, Eds., Academic Press, NY, 1976, p. 155.
52. Sokolov, A. P., Rossler, E., Kisliuk, A. & Quitmann, D. *Phys. Rev. Lett.*, 1993, **71**, 2068.